Journal homepage www.jzs.univsul.edu.iq
Journal of Zankoy Sulaimani
Part-A- (Pure and Applied Sciences)

Seismic Hazard Assessment of Northern Iraq

Ghassan I. Aleqabi[1] & Hafidh A. A. Ghalib[2]

1 Washington University in Saint Louis, Campus Box 1169, One Brookings Drive, Saint Louis, MO 63130, USA.
E-mail: ghassan@mantle.wustl.edu
2 Array Information Technology, 5130 Commercial Drive, Suite B, Melbourne, FL 32940, USA.
E-mail: hafidh.ghalib@arrayinfotech.com

Article info

Original: 6-10-2015
Accepted: 1-4-2016
Published online: 1-5-2016

Key Words:
Seismic
Hazard
risk
probability
PSHA

Abstract

Seismic hazard assessment is the estimation of the likelihood that an earthquake will occur in a given geographic area, within a particular window of time, and that it develops ground motion acceleration or intensity at a specific place within a specific area that exceeds a given threshold. It can be used as a tool for rational planning and designing in seismically active areas. For seismic hazard quantification, statistical analyzes of earthquake catalogs of northern Iraq and surrounding regions are carried out to estimate the rate and spatial distribution of earthquake events as a function of the magnitude and geographical location. Most techniques for estimating the likelihood of occurrence within a particular area are based on historical data of that region. An essential step in characterizing seismic hazards in an area is to determine the frequency and location of past earthquakes. Earthquakes tend to cluster around the most active faults. Kernel density estimators using a Gaussian kernel are applied to assess seismic hazard in the area. We performed Probabilistic Seismic Hazard Analysis (PSHA) to quantify the probability of exceeding a given ground motion in the area. The highest probability of seismic hazard exists in the northeastern part of Iraq and the Zagros regions. The seismic hazard is lowest to the west and south of northern Iraq, in the Mesopotamian valley. The comparison between the obtained results and the seismotectonic models of Iraq reveals that the current distribution of regional earthquakes agrees with the seismotectonic provinces of Iraq.

Introduction

Earthquakes are natural phenomena that occur randomly throughout history all over the world. They cause less loss in comparison with other natural disasters, like flood and the wind, but estimating the likelihood of occurrence of earthquakes is always hindered by significant uncertainties in estimating the sizes, locations, time and frequency of recurrences of future greater earthquakes [1]. The current rate of population growth, accompanied by the increasing number and complexity of infrastructure assets (buildings, bridges, dams, power plants, etc.), in addition to our extreme dependence on those structures, make modern societies vulnerable to future earthquakes. It is, therefore, necessary and important to evaluate the fundamental principles that form the basis of the seismic hazard for currently developed regions such as Kurdistan Region of Iraq (KRI). Probability analyzes are well developed for many of the forecasting problems in seismology. Using recent earthquakes rates (catalogs) at a particular region may provide answers on the likelihood of future earthquakes' occurrence within some time interval. However, seismic hazard data must be obtained by mathematically combining models for the location and size of potential future earthquakes with predictions of

the potential shaking intensity or peak ground acceleration caused by these future earthquakes. The mathematical approach for performing this calculation is known as Probabilistic Seismic Hazard Analysis (PSHA).

The probabilistic assessment of the seismic hazard for KRI will involve determining the ground motion that has a specified probability of being exceeded over a particular period. Accordingly, the output of the hazard analysis of KRI is a hazard map that shows the estimated magnitude distribution of ground motion that has a particular exceedance probability over a specified period. The authors can begin carrying out PSHA for KRI after (1) identifying all earthquake sources capable of producing damaging ground motions, (2) characterizing the distribution of earthquake magnitudes (i.e., regional seismicity model), (3) choosing an attenuation model, which describes generally how earthquake ground shaking or intensity decreases with distance away from the earthquake source, and (4) combining uncertainties in earthquake size, location and ground motion intensity using probability theorems. The KRI region has not experienced severe earthquakes in recent times, but significant tectonic features bound it including the Arabian platform in the southwest, the Turkish plateau in the northwest, and the central Iran plateau in the northeast. This is a region of significant tectonic settings such as abduction, and collision that is still ongoing along the northeastern boundary of the Arabian Plate. Active convergence has produced the Zagros and Bitlis sutures, which trend NW–SE along the Iraq-Iran border and E–W along the Iraq-Turkey border. The developed stress regime is the principal cause of earthquakes in areas surrounding the KRI, and it is also known from historical sources over the last millenniums. Earthquakes that affect KRI are mainly associated with collisions of the Arabian plate with the Eurasian plate. Small- to moderate-sized earthquakes frequently occur in Kurdistan, but the principle source of major earthquakes that affect KRI lies beyond the north and eastern borders of Iraq. While KRI exhibits low seismicity, it is adjacent to regions that have seen rather moderate to high seismic activity in the past. In this study, we will statistically and spatially evaluate the modern seismicity of KRI and surrounding regions and attempt to quantify the earthquake hazard in the area. Hazard analysis is the process of estimating the ground motion at a site or area of interest based on the characteristics of surrounding seismic sources. The results of this study will help the local governorates develop policies to mitigate the risks caused by of earthquakes.

Data

Seismic data used in this study cover the region between 29^{o}N - 41^{o}N and 39^{o}E - 51^{o}E. The data are obtained from the Advanced National Seismic System (ANSS) for the period 1924–2006 and magnitude $M \geq 3.5$, (http://earthquake.usgs.gov/earthquakes/search/) and from the North Iraq Seismographic Network (NISN) catalog for the period 2006–2009 and magnitude $M \geq 3.5$.

Seismicity and Tectonics of KRI

Information on the occurrence of historical earthquakes and knowledge of the various tectonic features that can be implicated in causing earthquakes are two main ingredients in seismic hazard analysis. In this analysis the KRI seismicity should not be isolated from the seismicity of surrounding regions, since it is by itself a low seismicity area. *Figure: 1* shows a seismicity map of Iraq. Small to moderate intra-plate earthquakes occur within the KRI region. The stress field in the area is a consequence of a major collision between the Arabian and Eurasian plates in Eastern Turkey that produced the 2 km high Anatolian-Iranian plateaus. The collision in Eastern Turkey is partially accommodated by the westward motion of the Anatolia Block along two faults, the North Anatolian Fault (NAF) and the East Anatolian Fault (EAF). Regarding the compressional stress regime orientation, the collision produces a field with two directions along the Bitlis-Zagros suture zone. One is perpendicular to the zone along Iraq-Iran border and the second is alternating between parallel and perpendicular to the suture zone along the Iraq-Turkey border *[2]*.

Iraq has a well-documented history of seismic activity. Sources for the seismicity of the area are historical records, modern earthquake data from international agencies, and recent instrumental measurements of seismicity of the KRI that were recorded by installing ten broadband seismic stations in the area to form the

Northern Iraq Seismographic Network (NISN) *[3]*. Earthquake activity in this region and surrounding areas is attributed to the well-defined Zagros fold-and-thrust belt. The north and northeastern (KRI) region is marked by the highest seismic activity in Iraq, with less activity in the south and southwestern part of Iraq. The convergence along the Arabian platform boundary in eastern and northeastern Iraq is still ongoing and causes stress accumulation that is evident by current seismic activity, and so the potential for producing relatively large destructive earthquakes cannot be ignored in this area.

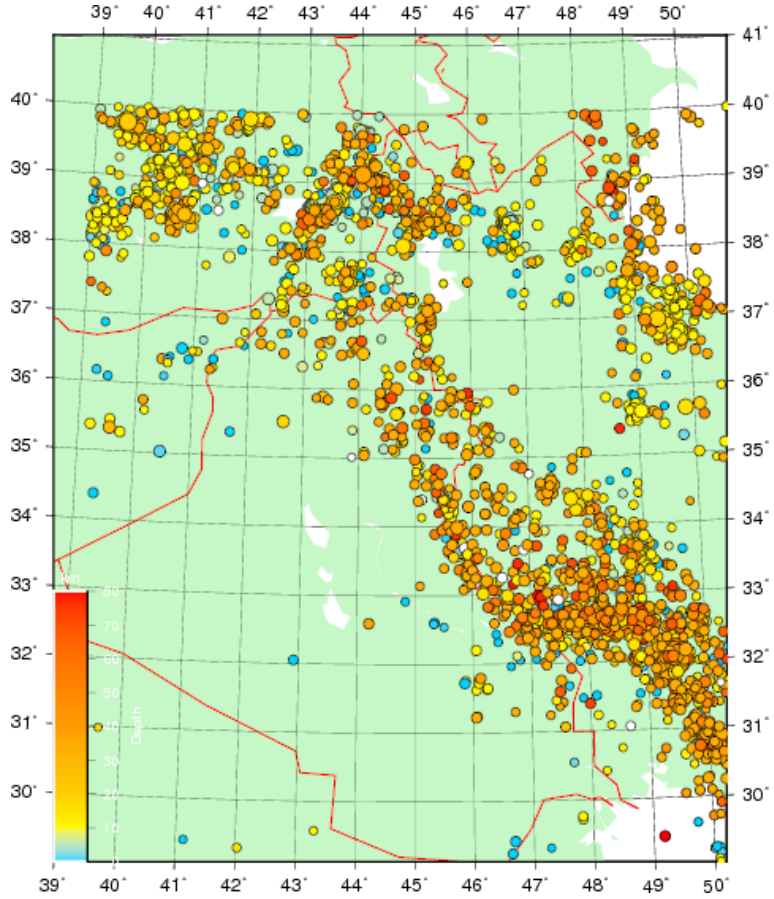

Figure-1: Seismicity map of Iraq and surrounding regions is showing earthquakes (circles) with magnitude >3.5. The radius of the circles indicates the magnitude, and the color of the circles reflects the depth of the earthquakes. This map depicts the seismicity of Iraq between 1924 and 2015.

Earthquake Probability (What We Can Learn from Earthquake Catalogs)

The probability of destructive earthquakes is low, and their recurrence is infrequent, but when it happens, the consequences are dire regarding lost lives and resources. Because of the infrequent occurrence of earthquakes in KRI, it is often difficult to plan for large earthquakes and build a reliable forecast of future activity because of lack of data, but this by no means should deter our attempts to conduct seismic hazard assessment, that involves extracting the most information possible from even inadequate and incomplete data sets such as earthquakes catalogs. To remedy data limitations, probability analysis is the preferred tool for forecasting the likelihood of future earthquakes within a given time interval, given past earthquake rates. It is advantageous to plot a histogram of the data (*Figure: 2*) to learn more about the quake recurrence rate.

This cumulative histogram (*Figure: 3*) shows a clear increase in the number of earthquakes after 1970 due to improved reporting of earthquakes in the latest part of the twentieth century. The recurrence rate of earthquakes seems almost constant until 2000 when the rate increased dramatically. This increase in seismic activity might not be attributed totally to improve earthquake recording but could at least in some part reflect increased seismic activity due to changes in the overall stress regime in KRI and surrounding regions. As was

noted above, the improved reporting of earthquakes in the decade after 2000 is due to the local installation of new broadband seismic stations.

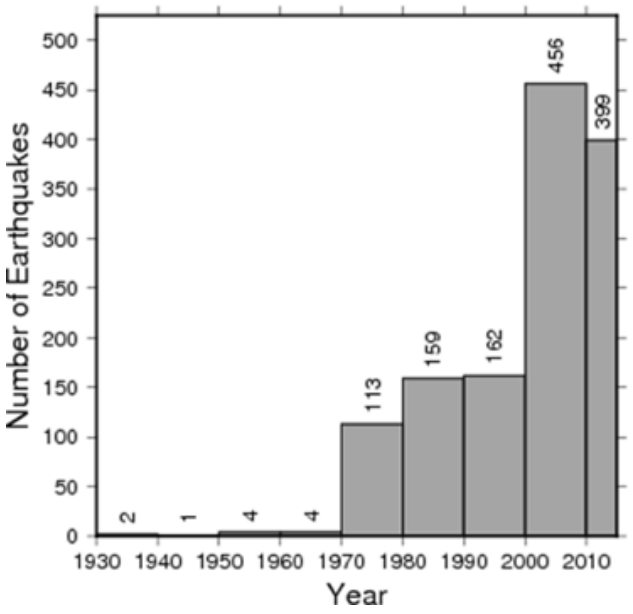

Figure-2: Histogram showing the distribution of earthquakes (magnitude > 3.5) in 10 y intervals. The total number of events in each interval displayed above the year bin.

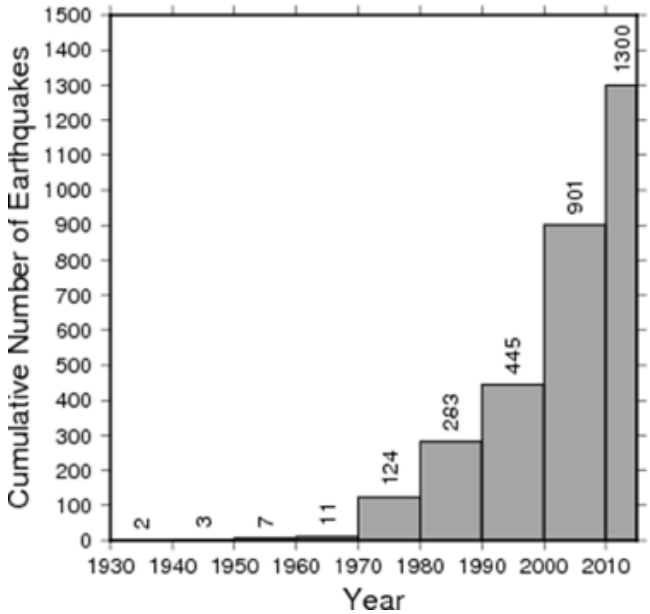

Figure-3: A cumulative number of earthquakes with magnitude > 3.5 in Iraq and surrounding regions plotted against time.

The earthquake recurrence rate could be estimated from seismicity data. For earthquakes with magnitude > 3.5, we have 36 events per year. This is an overall value, and it is not sensitive to the variations in geography and variations in the rate of seismic activity. The hazard curve (*Figure: 4*) is constructed to calculate the probability that the time between occurrences of earthquakes exceeds some duration; it assumes a Poisson model in which earthquake occurrences are independent in time. We estimated the hazard curve by calculating the interval between earthquakes in the data set and converting the calculated time interval into probability. The hazard curve is useful for evaluating the frequency of past earthquakes and is a guide to the

likelihood of future earthquakes. *Figure: 4* shows that there is between 80% - 100% exceedance probability that low-magnitude earthquakes will frequently occur in the region.

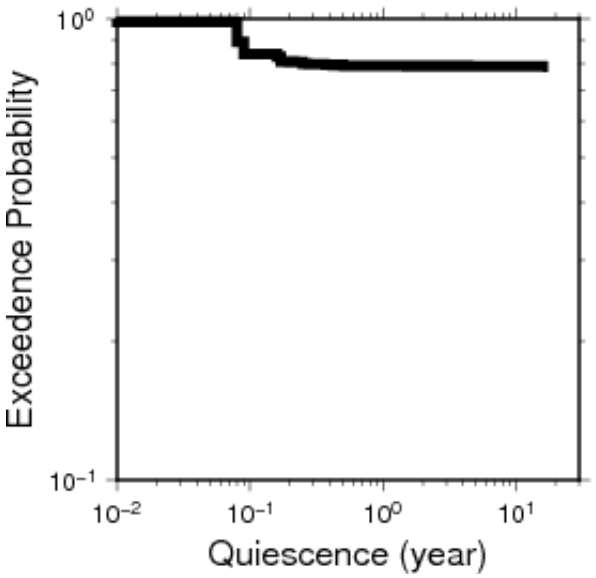

Figure-4: Hazard curve with exceedance probability.

Magnitude-Frequency Distribution

Gutenberg and Richter *[4]* expressed that the earthquake populations in a given region and period approximately follow the relationship $\log N = a - b\,M$. This is a power-law equation where N is the cumulative annual number of earthquakes whose magnitude exceeds M and where a and b are constants. For the majority of earthquake catalogs, the constant b is approximately equal to 1 ± 0.2, and it is a measure for the relative occurrence of large earthquakes versus small ones, since a small b-value implies a relatively large number of big earthquakes. The diagram of the equation above (*Figure: 5*) shows how many earthquakes of a given magnitude there are in a population of earthquakes and the probability of an earthquake with magnitude larger than M to occur anywhere in the region. *Figure: 5* is constructed for a region that is bounded between 29°N - 40°N and 40°E - 47°E and for earthquakes with magnitude greater than 3.5. It displays the $log_{10}(N(M))$ as a function of M. The linear regression yields a b-value (slope) of 0.825 and a-value (intercept) of 4.22.

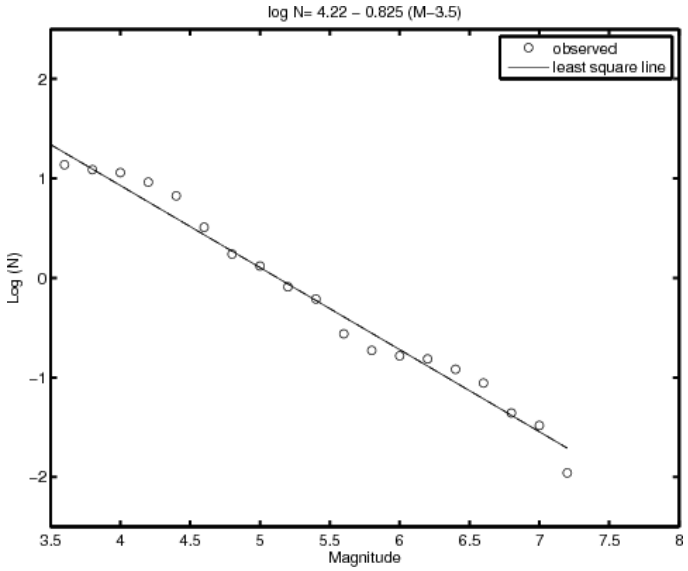

Figure-5: The observed allocation of the cumulative number of earthquakes per year of given magnitude, for earthquakes in KRI and surrounding regions with magnitude > 3.5.

Spatial Analysis of the Distribution of Earthquakes

Many spatial analyzes use a kernel density to smooth out the information represented by a collection of points that samples large areas (*e.g.*, earthquake distribution). Spatial analysis is necessary for hazard assessment in estimating how likely it is that an earthquake will occur at any particular location. Earthquakes can be considered as a point source processes with far-reaching effects over vast areas. Earthquake occurrence is not random in space since they tend to cluster around active faults and large plate margins. The current spatial distribution of earthquakes in KRI and surrounding areas is not uniform (*Figure: 1*), and some areas can be seen to have earthquake density greater than elsewhere. Estimation of the spatial distribution (kernel density) would provide a means to calculate the probability surface from the location of past events. Density estimators are sensitive to the spatial pattern of events (*i.e.*, the point distribution of earthquakes). These estimators take the point process distribution and construct a surface that reflects the likelihood of an event's occurring in each cell if it, in fact, occurs at all. For the KRI region we use a Gaussian kernel of the form:

$$G(x;\sigma) = \frac{1}{2\pi}\, e^{-\frac{1}{2}\left(\frac{x}{\sigma}\right)^2} \tag{1}$$

where x is the distance between a point q on the map to the i-th earthquake, and where σ is a smoothing parameter that determines the width of the Gaussian kernel. We obtain the expected density of future earthquakes γ, about a point q, by summing the kernel values G as follows:

$$\gamma\,(q) = \frac{1}{n\,\sigma^2} \sum_1^n G \tag{2}$$

where, n is the previous number of earthquakes that are used to estimate $\gamma(q)$.

The result of a density analysis is shown in Figure: 6, and it could be interpreted as a predictive risk surface for earthquakes in the future, assuming that the underlying stress regime that contributes to earthquakes occurrence will not change. Dark brown- to red-colored cells have more points (high risk) in them than lighter colored cells (yellow). From this perspective, earthquakes are random and can occur anywhere, but they are more likely to occur in certain areas, where consequently the risk of earthquakes is high.

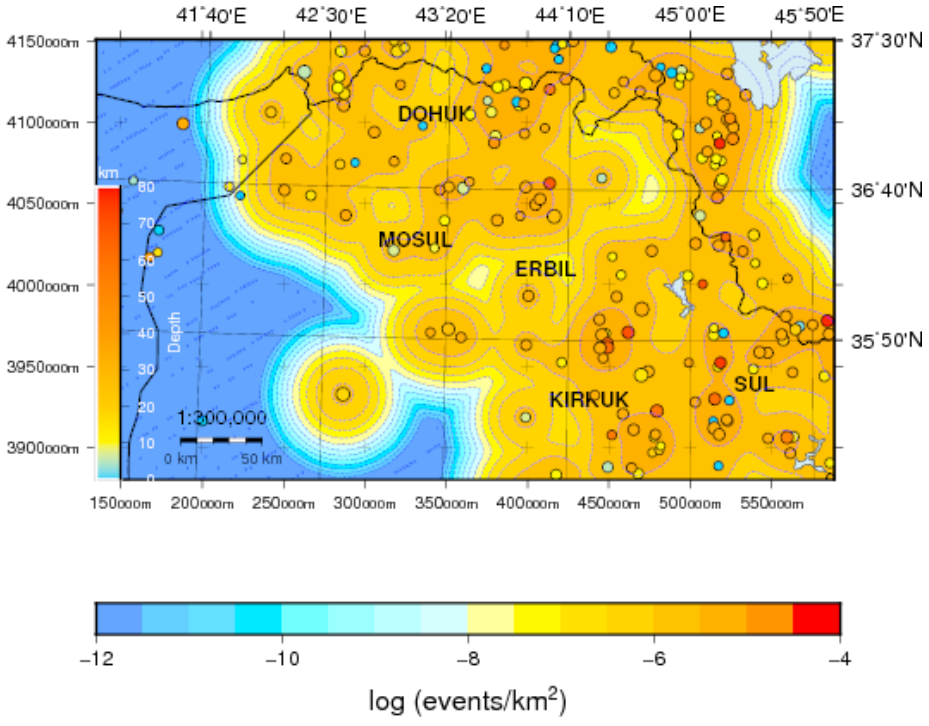

Figure-6: Probability surface of earthquake density, computed using $\sigma = 10{,}000\ m$.

Peak Ground Acceleration Attenuation Relationships

It is useful to have a crude estimate of Peak Ground Acceleration (PGA) attenuation with distance from the earthquake epicenter. The PGA relationships are predictive and depend on the earthquake magnitude and the distance to the quake epicenter or focus. Those formulas live in the realm of assumptions, so they come with high uncertainty. For depicting the earthquake ground motion we used the predictive empirical relationship for PGA *[5]*. The PGA map for KRI and surrounding regions is shown in *Figure: 7*. The PGA formula used is:

$$a_g = 472\ x\ 10^{0.28M}\ (R + 25)^{-1.3} \tag{3}$$

where, a_g is PGA in gals, M is the earthquake magnitude, and R is the distance to the earthquake.

Figure: 7 shows results using one formula from among many, including the one used in this study, that were developed for different regions with completely different geologic environments. Therefore, this map gives only a rudimentary description of the PGA attenuation with distance for events with magnitude greater than 6. The contour line of $0.1g$ is plotted; this corresponds to a value that causes considerable damage in poorly built structures.

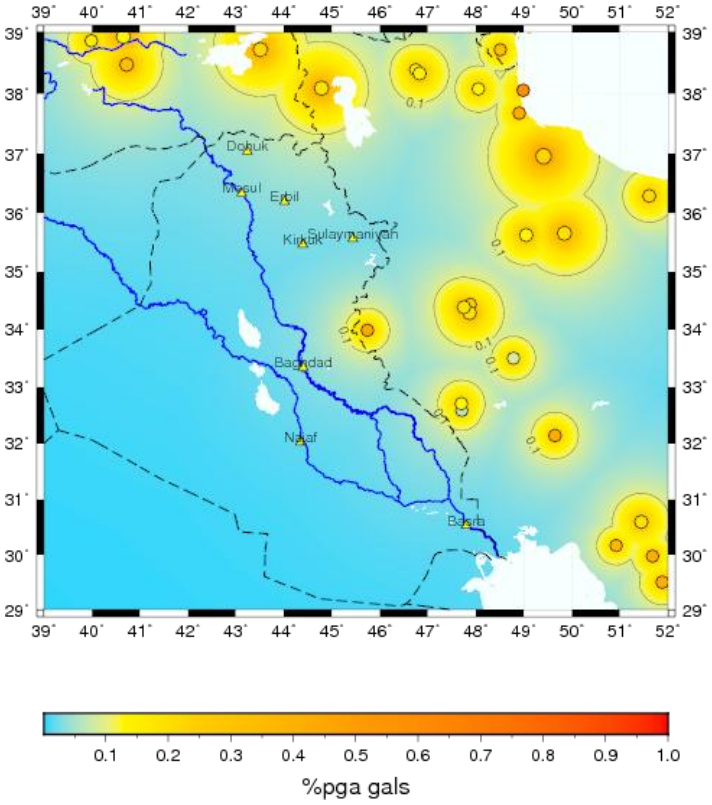

Figure-7: An example of PGA map constructed for the KRI and surrounding regions, for earthquakes having magnitude 6 and above.

Probabilistic Seismic Hazard Analysis (PSHA)

It is important to mention that the probabilistic seismic hazard is described as the level of ground shaking that has a certain chance of being exceeded in a given period at a site, based on the characteristics of surrounding seismic sources. Cornell introduced the PSHA methodology *[6]* and McGuire *[7]*, and it is based on three key models, specifically (1) seismicity distributions, (2) frequency-magnitude distributions, and (3) ground motion prediction equations:

1. Earthquake Sources Determination (Seismicity Distribution)

Regions that generate earthquakes are called "earthquake source zones." Seismic sources are regions that have experienced earthquake activity in the past and serve as potential sources of future earthquakes. Seismic sources are delineated based on seismotectonic features of the area, and it is assumed that the past and current earthquake activity is a reliable predictor of the future seismic activity. Generally, and for the sake of seismic hazard analysis, several earthquake source zones are defined with their level of activity determined from both current and historical seismicity and an understanding of the underlying geological structures. From the seismicity map (*Figure: 1* and *Figure: 8*) The authors can identify six earthquakes source zones (*Figure: 8*) around KRI. The choice of seismic source regions is subjective, and in our case, it is assumed that the

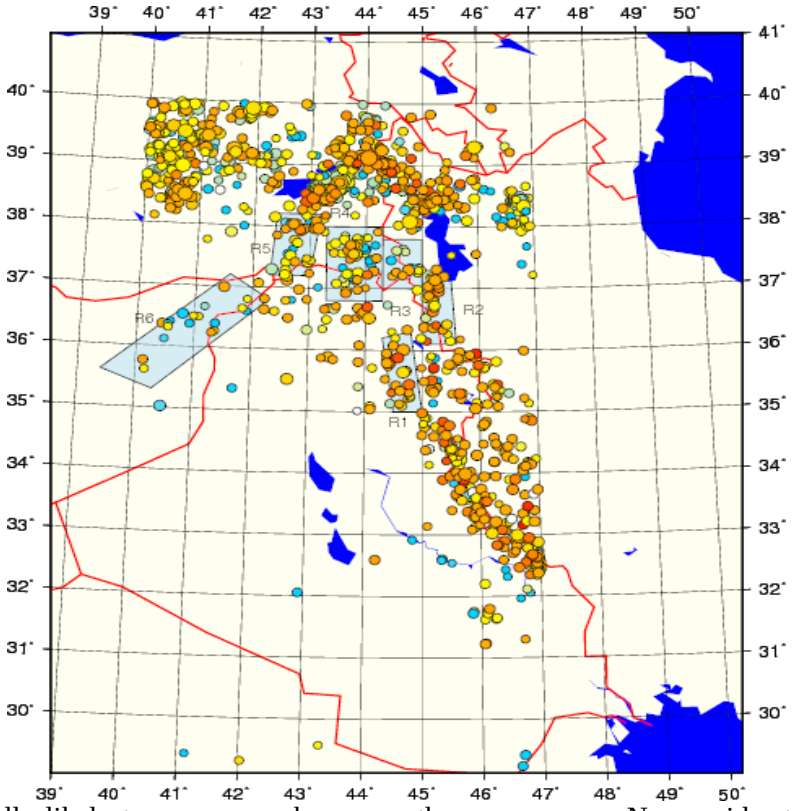

earthquakes are equally likely to occur anywhere over the area source. No consideration was given to the specific geophysical, geological, and tectonic characteristics of the area other than the seismicity distribution.

Figure-8: Seismic source zonation used in this study. Six zones were chosen and marked on the map from R1 to R6.

2. Regional Model of Seismicity (Frequency-Magnitude Distribution)

PSHA requires an earthquake probability distribution function that describes the earthquake recurrence relation for each seismic region. For each chosen seismic region it is assumed that there is a pair of parameters *a* and *b* of the Gutenberg-Richter magnitude-frequency distribution $log_{10} N_m > M = a + bM$, where N is the annual cumulative number of earthquakes greater than magnitude M, and where a and b are the regression parameters that describe the earthquake recurrence relationship for a given seismic zone (*Figure: 5* and *Figure: 8*). The *a*-value is the intercept of the curve in *Figure: 5*, and it represents the rate of occurrence of all events larger than 3.5. It will be a challenge to assign an activity rate to the selected seismic zones in *Figure: 8*, since we did not use all the seismicity in the zone in finding the *a* value and *b*-value. Therefore, we assigned an activity rate as a percent of the total activity based on the number of events in each source zone. The *b*-value determined from the whole dataset is assigned to each zone in Fig. 8, since it is assumed that significant uncertainty values will be attached to an individual zone's *b*-value on account of the limited data set for each zone. For a given source zone, PSHA calculation requires the selection of minimum and maximum magnitude values. For all the regions, the minimum magnitude is equal to 3.5 and the maximum

magnitude is equal to 6.5. Shallow earthquake depths (10 km) are assigned to all six source zones. The background seismicity rate is the sum of all the zones' rates. *Table 1:* lists the values of all parameters for each zone.

Table 1: Seismic parameter values for the chosen earthquake zones surrounding KRI.

Zone	M_{min}	M_{max}	$b\ ln(10)$	*Seismicity rate*
1	*3.5*	*6*	*1.9*	*0.065*
2	*3.5*	*6*	*1.9*	*0.075*
3	*3.5*	*6*	*1.9*	*0.040*
4	*3.5*	*6*	*1.9*	*0.114*
5	*3.5*	*6*	*1.9*	*0.075*
6	*3.5*	*6*	*1.9*	*0.060*
Background	*3.5*	*6*	*1.9*	*0.430*

3. Attenuation Relationships

To determine the seismic hazard at a certain site, an estimate is needed of the ground motion caused by an earthquake of a particular magnitude at a given distance. For this purpose, many attenuation models have been developed that predict ground motion at a certain site due to an earthquake at a distance from the site (*Figure: 7*). The attenuation model of McGuire *[5]* has been used in this study and is described as

$$\ln\ \mathrm{A} = C_1 + C_2\ \mathrm{M} + C_3\ \ln(\mathrm{R} + 25) \tag{4}$$

where *ln A* is the peak ground acceleration in gals, C_1, C_2 and C_3 are constants having the values 6.16, 0.64 and -1.30 respectively, M is the earthquake magnitude, and R is the distance from the earthquake to the site. No site response model is used to adjust the earthquake ground shaking at a site for the influence on the propagating seismic waves of weathered rock and overlying soils.

PSHA Calculations for KRI

References *[6]* and *[7]* assumed the overall hazard at a site comes from the effects of all possible magnitudes and distances (from a total of *N* seismic sources), and they combine the probabilities of occurrence into a single seismic hazard estimate, such that $E(Z)$ is the expected mean annual rate of occurrence of earthquakes (mean annual expected number) that cause an amplitude Z to exceed a threshold amplitude z. The seismic hazard estimate can be expressed as

$$E[Z > z] = \sum_{i=1}^{N_{sources}} \lambda_i \int_{m_{min}}^{m_{max}} \int_{r_{min}}^{r_{max}} P(Z > z|m,r)\,.\,f_i(m).\,g_i(r).\,dm\,d \tag{5}$$

where λ_i is a scaling factor representing the annual rate of earthquakes exceeding a lower bound on the earthquake magnitudes for the *i*-th source; $P(Z > z|m,r)$ is the conditional cumulative distribution function, defining the probability that the threshold value z of the ground motion amplitude is exceeded under the condition that an event of magnitude m occurred at distance r; $f_i(m)$ is the probability density function for magnitude that is derived from the earthquake frequency-magnitude distribution; $g_i(r)$ is the source-site density distribution indicating the probability that an earthquake occurs at a distance r from the site (zonation); and m is local magnitude. The probability that amplitude Z occurs depends on $f_i(m)$ and $g_i(r)$.

The data sources used in this study were identified in the data section. The analytical equations of the Probabilistic Seismic Hazard Analysis (PSHA) method of Cornell *[6]* are numerically approached in the program EQRISK *[7]*. In this study, EQRISK is used to model the seismic hazard for the KRI, a small seismicity region. The input parameters, (*Table 1*, zonation, magnitude-frequency relation, ground motion prediction equation, and depth of seismicity) are determined from the most recent earthquake catalog and the literature. To gain insight into the pattern of seismic hazard, we have computed the seismic hazard for a large number of sites within the area. Using the EQRISK program, values of the probabilistic ground shaking

thresholds (the Peak Ground Acceleration [PGA]) that have a 10% probability of being exceeded in 50 years have been developed for all 1ox1o areas of KRI and surrounding areas (*Figure: 9*).

Probabilistic hazard maps like the one in *Figure: 9* are typically expressed regarding the probability that a certain ground motion will be exceeded. The map is showing a 10% probability of exceedance in 50 years depicts thresholds with an annual probability of 1 in 475 of being exceeded each year. This level of ground shaking has been used for designing buildings in high seismic areas. *Figure: 9* shows a 10% probability of exceedance in 50 years, so it displays the ground motions that have a 90% chance of not being exceeded in the next 50 years. This probability level allows engineers to design buildings for larger ground motions than what we think will occur during a 50-year interval, which will make buildings safer than if they were designed for only the ground motions that we expect to occur in the next 50 years. According to *Figure: 9*, it seems that the seismic hazard in the northeast part of the map is dominated by nearby seismically active source regions. Since limited data are available for the KRI, the seismic hazard analysis performed in this study admits to a wide range of interpretations and uncertainties. The authors have not yet investigated the sensitivity of the hazard estimate to the input parameters. It is anticipated that the hazard estimate would be sensitive to the definition of source zonation and the choice of ground motion prediction equation. Both source zonation and ground motion prediction require the application of more seismological, geological, and geophysical knowledge. For this study, soil type was assumed to be same for all the source zones. It is known that soil type and local site conditions influence hazard estimates, so we anticipate that much improvement in hazard values can be achieved by introducing into the model more constraints based on local geology. The addition of more seismicity data also cannot be overlooked in producing refined hazard estimates.

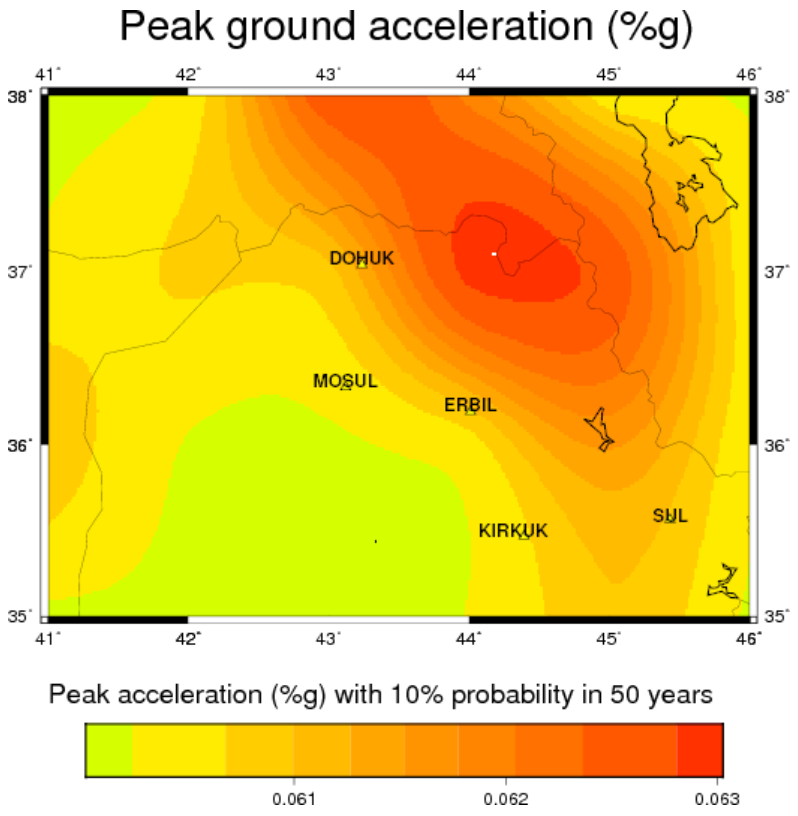

Figure-9: The map that shows the hazard from earthquakes that could occur in KRI and surrounding area. It is probabilistic in the sense that the analysis takes into consideration the uncertainties in the size and location of earthquakes and the resulting ground motions that can affect a particular site. The unit g is the acceleration of gravity. The information shown on this map is not to be used for site-specific seismic hazards analyses, but it illustrates the general regional patterns of the shaking hazard.

Discussion and Conclusions

This paper conducts seismic hazard calculations for KRI and surrounding regions. From the earthquake

catalog, the authors constructed a histogram of seismic magnitudes by years and a cumulative histogram. On the histograms, it is clear that the frequency of earthquakes was less before the year 2000, with a clear increase after 2000. This seems to indicate much-improved seismic event reporting, starting with the installing of the NISN in northern Iraq. The recurrence rate of earthquakes looks fairly constant during the three decades prior to 2000 and the next two decades after 2000. Once again, in the 2000's there appears to be a reasonable increase in activity that might not be entirely attributable to improved event reporting. Perhaps this indicates a change in the seismic activity. The hazard curve is useful for evaluating the frequency of past earthquakes and is a guide to the likelihood of future earthquakes. The probability that the interval between earthquakes is less than one year in duration at KRI and surroundings is about 80%. The inverse of the repose period between earthquakes is the recurrence rate. Therefore, from the hazard curve, we know that there is 80% chance that the seismic activity at KRI and surroundings is greater than one event/year. The resulting magnitude-frequency statistic for KRI and surroundings exhibit a constant b-value of 0.825. The spatial density distribution of earthquakes is estimated using the Gaussian equation. We notice two narrow corridors exist where earthquake probability is low.

PSHA analysis is based on the probability of ground accelerations exceeding 50 gals over 50-year period. In general, the northeastern parts of KRI, including Duhok, have the highest expected peak ground acceleration. Future research is required to develop a local attenuation relation of PGA with distance and earthquake magnitude. In interpreting the results, it should be noted that the "probabilities of exceedance" calculated for crustal earthquakes are not probabilities of earthquake occurrence; rather they are probabilities of certain ground acceleration being exceeded at specific locations with uniform firm ground conditions. Therefore, because of site conditions, these probabilities would be higher for softer ground. However, quantifying the effect of variations in ground conditions is not intended in this paper. The exceedance probabilities are given for a certain time interval and are time-independent, i.e., the passage of time will not affect those probabilities due to the Poissonian probability models used in the calculations. Furthermore, in the KRI, and particularly the southwestern part, the probabilities are low, but it is still recommended to have a comprehensive plan for earthquake preparedness, response, and recovery for the area. Finally, while every effort was made to quantify and present KRI's earthquake hazard information in easy-to-understand terms, the authors consciously did not assign any hazard levels such as low, medium, or "high" hazard to any part of KRI and surroundings. As a result, it is left to the communities to determine their respective tolerances to the earthquake hazard, risk and vulnerability in their area of responsibility.

Acknowledgments

The authors thank Kurdistan General Directorate of Meteorology and Seismology for supporting the project. Wilmer Rivers and Florence Martin are appreciated to editing the text of this paper. The maps and graphs in this article were created using the Generic Mapping Tools *[8]*.

References

[1] Lee, V. W., "On Strong Motion Uniform Risk Functionals Computed from General Probability Distributions of Earthquake Recurrences", Int. Journal of Soil Dynamics and Earthquake Eng., Vol. (11), No. (6), pp. 357-367. (1992).

[2] Abdulnaby, W., Mahdi, H., Numan, N., and Al-Shukri, H."Seismotectonics of the Bitlis–Zagros Fold and Thrust Belt in Northern Iraq and Surrounding Regions from Moment Tensor Analysis", Pure and Applied Geophysics, Vol. (171), No. 7, pp. 1237-1250. (2014).

[3] Ghalib, H. A. A., Aleqabi, G. I., Ali, B. S., Saleh, B. I., Mahmood, D. S., Gupta. I. N., Wagner, R. A. , Shore, P. J., Mahmood, A., Abdullah, S., Shaswar, O. K., Ibrahim, F., Ali, B., Omar, L., Aziz, N. I., Ahmed, N. H., Ali, A. A., Taqi, A.-K. A., and Khalaf , S. R.C.M.P. "Seismic characteristics of northern Iraq and surrounding regions", in Proceedings of the 28th Seismic Research Review: Ground-Based Nuclear Explosion Monitoring Technologies , LA-UR-06-5471, Vol. 1, pp. 40–48. (2006).

[4] Gutenberg, B. and Richter, C. F. "Seismicity of the Earth and Associated Phenomena", 2nd ed., Princeton Univ. Press, pp. 310. (1954).

[5] McGuire, R. K. "Seismic structural response risk analysis, incorporating peak response regressions on earthquake magnitude and distance", Mass. Inst. Tech., Dept. of Civil Eng., Publication No. 399, p. 371. (1974).

[6] Cornell, C. A. "Engineering Seismic Risk Analysis", Bulletin of the Seismological Society of America, Vol. (58), No. 5, pp. 1583-1606. (1968).

[7] McGuire, R. K."FORTRAN computer program for seismic risk analysis", U.S. Geol. Survey Open-File Rep., 76-67, p.90. (1976).

[8] Wessel, P., and W. H. F. Smith, New, improved version of Generic Mapping Tools released, EOS Trans. Amer. Geophys. U., vol. 79 (47), pp. 579, 1998.